Modeling future dissolved oxygen and temperature profiles in small temperate lake trout lakes

Aidin Jabbari[1,2,*], Leon Boegman[1] and Lewis Molot[3]

1. Environmental Fluid Dynamics Laboratory, Department of Civil Engineering, Queen's University, Kingston, ON, Canada

2. Present address: National Institute of Water and Atmospheric Research, Christchurch 8440, New Zealand

3. Faculty of Environmental and Urban Change, York University, Toronto, ON, Canada

* Corresponding author: Aidin.Jabbari@niwa.co.nz

ABSTRACT

Climate warming has been projected to alter the habitat ranges of cold-water fish species. To numerically model these changes, a simple dissolved oxygen (DO) sub-model has been embedded into a one-dimensional thermodynamic lake-tile model that simulates small unresolved lakes within the land surface scheme of a climate model. To account for the lack of monitoring data for most small lakes, respiration, photosynthetic production, and sediment oxygen demand were parameterized as functions of simulated light intensity, water temperature and the DO concentration. The model predicted the temperature and DO profiles with root-mean-square error <1.5 °C and <3 mg L^{-1}, respectively, in two Canadian Boreal lakes. Simulations of future (2071-2100) lake conditions predict a warming-induced reduction in the strength of seasonal lake turnover events occurring for RCP 2.6, and consequently long periods of hypolimnetic hypoxia. Further reductions in DO for RCP 4.5 and 8.6 were negligible. This will reduce the end-of-summer volume weighted hypolimnetic dissolved oxygen concentration from ~6 mg L^{-1} during 1978-2005 to ~1 mg L^{-1} during 2071-2100 (average of 3 RCPs), well below the 7 mg L^{-1} provincial standard for juvenile lake trout.

Introduction

Small lakes on the Canadian Boreal Shield provide habitat for cold-water fish species, including lake trout (*Salvelinus namaycush*), whose populations are becoming increasingly threatened from multiple stressors (e.g., climate change, eutrophication, shoreline development and over-exploitation; (Guzzo & Blanchfield, 2017; Nelligan et al., 2016; Sharma et al., 2009). Observed declines in deep-water dissolved oxygen (DO) concentrations, in lakes where nutrient inputs have remained steady or decreased (e.g., (Nelligan et al., 2016; Summers et al., 2012), raise the level of concern about climate warming as a threat-multiplier (Smol, 2010). For instance, from 1980 to 2008 in Lake Simcoe, Stainsby et al (2011) observed a long-term trend of earlier thermal stratification onset and increased stratification duration from warmer air temperatures. This has been simulated to cause a ~2 mg L^{-1} decrease in summer deep-water DO over the next 100 years (Bolkhari et al., 2022). The increased thermal stability, from climate warming, is also expected to inhibit deep-mixing during turnover periods (Jankowski et al., 2006; Schwefel et al., 2016; Woolway & Merchant, 2019), reducing the degree to which spring and fall turnover events re-oxygenate the hypolimnion (Boegman et al., 2012; Yang et al., 2017), which is a key factor in predicting end-of-summer DO in temperate lakes (Ghane & Boegman, 2023; Molot et al., 1992; Nakhaei et al., 2021). Increased thermal stability and reduced spring mixing couple to negatively impact the availability of oxygenated habitat for cold-water fish such as lake trout (Ficke et al., 2007).

To fully evaluate the impacts of future climate change on both the thermal structure and deep water DO, lake models must be developed that are integrated within the land surface schemes of climate models (MacKay et al., 2009). However, the vast majority of lakes, in such a modelling system, would be unresolved (< ~50 km regional climate model grid scale). To overcome this, these lakes may be uniquely represented as 'lake tiles' that are simulated with one-dimensional (1D, vertical) models. MacKay (2012) developed a 1D bulk mixed-layer model, the Canadian Small Lake Model (CSLM), for simulation of the thermal structure in a climate model land-surface scheme (Garnaud et al., 2022; Verseghy & MacKay, 2017). Using surface meteorology derived from direct observations or from climate model output, the only variables controlling the simulated physical characteristics of lakes within the CSLM framework, are the light extinction coefficient, lake surface area and lake depth (MacKay et al., 2017). This allows for maximum computational efficiency and for general applicability to lakes with limited observational data; however, calibrating such a simple model with few adjustable parameters remains a challenge.

The objective of the present work is to develop a DO sub-model, with minimal calibration parameters, for inclusion into CSLM. This will allow for simulation of the future effects of climate change on stratification and hypoxia in lakes. We implemented and evaluated a DO sub-model using both mixed layer and turbulent diffusion approaches to transport DO vertically below the metalimnion of two Canadian lakes. Given the dependence of lake trout on DO and temperature profiles (Dillon et al., 2003), the models were then applied to simulate future impacts of climate change on lake trout habitat (i.e., temperature and DO distributions), between 1978-2005 and 2071-2100 under three climate change emission scenarios.

Methods

Study sites and observed data

The models were developed using long-term data sets from two Canadian lakes, which are separated by ~200 km (Fig. 1). Both lakes are deep and oligotrophic, with lake trout populations. Eagle Lake has historically been stocked with lake trout (periodically from 1917 to 1994; I. Dardick, Sept. 2015) to increase their abundance for anglers. Long periods of late summer hypolimnetic hypoxia have been reported in both lakes (Nelligan et al., 2016), and they have been classified as 'at capacity' (restriction of development with in 300 m of the shoreline) because the mean volume-weighted hypolimnetic oxygen concentration (VWHO) at the end-of-summer has been less than the provincial standard (i.e., 7 mgL^{-1} to support juvenile lake trout lake; Ontario Ministry of the Environment and Climate Change (OMOECC) 2011).

We recorded meteorological data at Eagle Lake (44° 41.5240' N, 76° 41.4370' W, maximum depth=30 m, $(\text{surface area})^{1/2}$ = 250 m) over 5 years (22 June 2011 to 29 July 29, 2015) with a tripod-mounted Onset HOBO U30 Weather Station on a small, isolated island at 10-min intervals. The instruments measured air temperature and relative humidity (STHB-M002; ±0.21°C, ±2.5% accuracy), shortwave radiation (S-LIB-M003; ±10 W m^{-2} accuracy), and 10-min average wind speed and direction (S-WCF-M003; ±1 m s^{-1}, ±7°) at a 2 m height. Profiles of water column temperature, DO and Secchi depth were available from the routine monitoring databases of the Ontario Ministry of the Environment Conservation and Parks (MOECP) and the Rideau Valley Conservation Authority (RVCA) at the deepest location in the lake during May through September (typically four profiles per year).

Harp Lake (45° 38' N, 79° 13'W, maximum depth 34 m, $(\text{surface area})^{1/2}$ = 843 m) meteorological data (8 June 1978 to 31 December 2007) were obtained from an extensive monitoring program by the MOECP (Yan et al., 2008). The weather station is located ~500 m west of the lake and has recorded air temperature, humidity, wind and solar radiation since 1970 (Yao et al., 2014). Records of ice phenology (ice-on, ice-off dates) have been collected since 1975 (Yao et al., 2013).

In both lakes, mean daily cloud cover (Fischer et al., 1979) was input each timestep, as calculated from daily averaged clear-sky radiation (clskswr.m) and measured shortwave radiation. Limnological parameters, including Secchi depth, total chlorophyll-a (integrated over 2 × Secchi depth) and temperature and DO profiles were collected every two weeks or monthly since 1978 during the open water season (usually from Apr/May to Oct/Nov). Predicted profiles of temperature and DO from the model were calibrated against 485 observed profiles in Harp Lake (1978-2007) and 20 observed profiles in Eagle Lake (2011-2015).

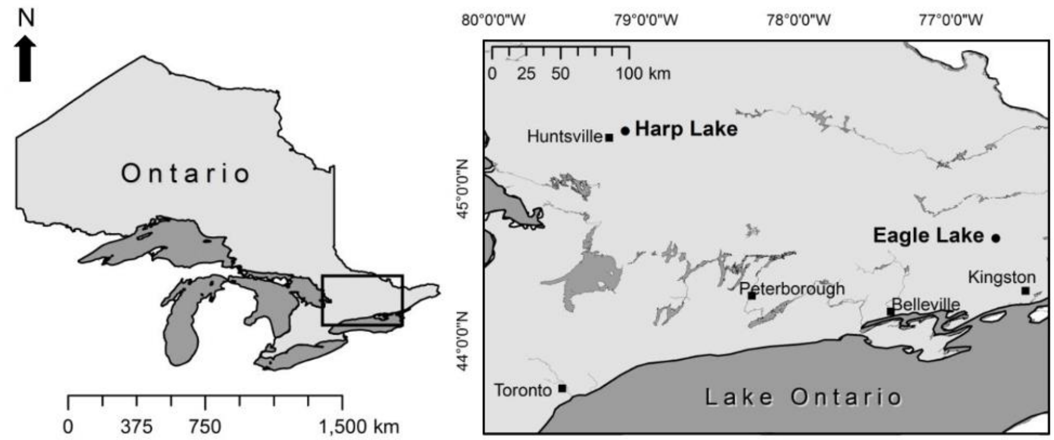

FIG. 1. The location of the observation data: Eagle Lake (44°40′ N 76°42′ W, maximum depth 30 m) and Harp Lake (45°38′ N 79°13′ W, maximum depth 34 m) in Ontario, Canada. Modified from Nelligan et al. (2016).

Climate model forcing:

To evaluate forcing-bias, when developing coupled lake-atmosphere models it is a requirement to test the accuracy of the lake model when forced directly with atmospheric (or climate) model output, in comparison to being forced with observed meteorological data (Huang et al., 2012; Hurtado et al., 2023). Consequently, simulation dates were selected based on the availability of both meteorological forcing data sets (observations and GCM model output) and water temperature calibration data. Three different scenarios were run: (1) with observed meteorological forcing (Eagle Lake: 2011-2015 and Harp Lake 1978-2007); (2) with GCM-generated 'baseline' meteorological data (1978-2005); and with (3) GCM-generated 'future' meteorological data (2071-2100). Simulations (1) and (2) were to assess the error in applying GCM forcing without downscaling and simulations (2) and (3) were to assess the impacts of climate change.

The GCM output is a statistical representation of the atmospheric conditions in each year, and thus does not necessarily capture the exact timing of individual meteorological events (e.g., the day of a large storm). Therefore, here we quantitatively compared mean seasonal statistics, as opposed to conventional variables, such as instantaneous profiles of temperature and DO.

Present day (1978-2005) and future (2071-2100) global climate model (GCM) forcing data were obtained from the simulations of the Canadian Earth System Model (CanESM2/CGCM4), which was run as part of CMIP5 with a 50-km grid resolution. The emission scenarios included the Representative Concentration Pathways 2.6 (RCP 2.6), 4.5 (RCP 4.5) and 8.5 (RCP 8.5). RCP 2.6 is a low greenhouse gas emission scenario in which changes to the radiative forcing would lead to an increase in the global mean temperature of 1°C. Under RCP 2.6, global emissions are projected to decrease to near zero by the end of 2100. Under the medium RCP 4.5 emission scenario, changes to the radiative forcing cause a 2 °C increase in air temperature under stabilized greenhouse gas emissions. For the high emission scenario RCP 8.5, changes to the radiative forcing result in an increase of 3.7 °C in the air temperature with a continuous emission growth

(IPCC, 2013).

Lake model description

The CSLM is a one-dimensional (1D) thermodynamic lake model that computes the response of the water column to atmospheric forcing in the form of surface wind stress, sensible and latent heat flux and long- and short-wave radiation. The surface mixed layer is computed using a turbulent kinetic energy budget (Imberger, 1985; Spigel et al., 1986), shortwave radiation penetrates the water column using Beer's Law and the equation of state follows Farmer and Carmack (1981). The snow and ice model includes the snowpack physics component of the Canadian Land Surface Scheme. Further details of the numerical scheme and parameterizations are provided in the literature (Garnaud et al., 2022; MacKay, 2012; MacKay et al., 2017; Verseghy & MacKay, 2017).

The model was applied to both lakes with a vertical grid resolution ∂z = 0.5 m and timestep ∂t = 10 min. The light extinction coefficients were determined to be 0.3 m^{-1} and 0.5 m^{-1} in Lake Eagle and Harp Lake, respectively, from calibration of the temperature profiles to minimize root-mean-square (RMS) error in comparison to the observed temperature profiles (Table 1).

Dissolved oxygen sub-model

A dissolved oxygen sub-model was added by including process parameterizations for the free-surface flux, sediment oxygen demand, photosynthetic production at constant nutrient inputs, hypolimnetic oxygen demand and hypolimnetic mixing. Vertical mixing below the surface mixed layer (h_S), was added to CSLM to diffuse the effects of the SOD, from the bottom boundary condition, through the water column. Two mixing algorithms were implemented and tested. In the first algorithm, the a bottom mixed layer (BML) thickness (h_B) was calculated (Imberger, 1985; Spigel et al., 1986):

$$\frac{d(uh_B)}{dt} = {u_B^*}^2 \tag{1}$$

where u is the mixed-layer velocity and u_B^* is the bottom friction velocity. Here, u_B^* was estimated from the surface friction velocity ($u_S^*, u_B^* = 0.2u_S^*$), which is calculated from the surface wind speed (Ivey & Patterson, 1984). This method assumes a uniform DO in the fully turbulent BML that results from stirring, shear and buoyancy production (MacKay, 2012) and has been found to reproduce hypolimnetic DO concentrations in Lake Erie (Ivey & Patterson, 1984). In the second algorithm, the DO flux (J) was computed from Fick's Law:

$$J = -K\frac{dDO}{dz} \tag{2}$$

where K is the turbulent diffusivity. From microstructure casts in Eagle Lake, we found K to be consistently (~10^{-7} m^2s^{-1}) through the hypolimnion (Ghane & Boegman, 2021; Nakhaei et al., 2016) and adopt this observed value in the present model.

The DO sub-model development follows that of DYRESM-WQ (Hamilton & Schladow, 1997). To first order, the hypolimnetic oxygen demand (HOD; sum of respiration, photosynthesis, nitrification and mineralization) and SOD affect the DO budget below the metalimnion. To model HOD, we tested two approaches: first HOD was constant through the water column (Bouffard et al., 2013; Ghane & Boegman, 2023; Nakhaei et al., 2021). From model calibration against the DO profile data, we found HOD = 0.03 g $m^{-3}d^{-1}$ and 0.08 g $m^{-3}d^{-1}$ for Harp Lake and Eagle Lake, respectively (Table 1).

In the second approach, we parameterized respiration as a fixed rate: 1.8 and 0.2 mg O_2 (mg Chl *a*)$^{-1}$ h^{-1} in the upper and bottom mixed layers, respectively (Table 1), obtained from calibration of the model to DO profiles from both lakes (Ganf, 1974; Gibson, 1975; Patterson et al., 1985). Photosynthetic production follows Platt et al. (1980), as a function of light intensity:

$$P^B = P_M^B\left[1 - \exp\left(-\alpha I / P_M^B\right)\right]\exp\left(-\beta I / P_M^B\right) \tag{3}$$

where P_M^B is the maximum potential specific productivity (41.5 mg O_2 (mg Chl *a*)$^{-1}$ h^{-1}; (Patterson et al., 1985)) and α and β are parameters: 0.1 and 4.2 mg O_2 (mg Chl *a*)$^{-1}$ h^{-1} (W m^{-2})$^{-1}$, respectively, obtained from calibration for both lakes (Table 1). Here, chlorophyll *a* was parameterized as a function of surface temperature (T_S) by fitting the fortnightly observed chlorophyll *a* concentration (1976-2015) to T_S in Harp Lake (Fig. S1):

$$\text{Chl } a = 0.001\left(0.00042T_S^3 - 0.0243T_S^2 + 0.461T_S\right) \tag{4}$$

The SOD was applied across the bottom boundary of the model cell above the bed and was calculated using a modification of the biochemical model (Walker & Snodgrass, 1986):

$$SOD = \left(\frac{DO}{DO + K_m}\right)\left(\frac{\eta_b \alpha_{sed}^{T-20}}{\mathrm{d}z}\right) \tag{5}$$

where η_b=0.46 gO_2 m^{-2} d^{-1} is the maximum biochemical sediment oxygen uptake (Bouffard et al., 2013; Nakhaei et al., 2021), K_m=1.5 mgL^{-1} is the half saturation constant for DO (Robson & Hamilton, 2004), α_{sed}=1.08 is the sediment temperature multiplier for release rate (Robson & Hamilton, 2004), and T is the water temperature.

Analytical methods:

We calculated VWHO as:

$$VWHO = \sum V_n DO_n / V_T \tag{6}$$

where V_T is the total volume of the hypolimnion and V_n and DO_n are the volume and DO, respectively, at depth n. Here, we define hypolimnion as the strata below the metalimnion layer where the vertical temperature gradient is < 1°C m^{-1} (Quinlan et al., 2005).

Results

Model Evaluation

When forced with observed meteorological data, we assessed the accuracy of the model in prediction of the 485 (Harp Lake; Fig. 2a) and 20 (Eagle Lake; Fig. 2c) observed temperature and DO profiles. The ice model was also compared to ~30 years of observed ice-on and -off dates from Harp Lake (Fig. S2). After manual calibration (Table 1), the model reproduced observed temperatures (e.g., Figs. 3a and 3e) with RMS error e_T < 1.6 °C (Figs. 3c and 3g) and 65% of the modelled ice-on and -off days were within ±5 days of the corresponding observations (Fig. S2). This provides indirect confirmation that model predictions of the length of stratification are reasonable.

The model-calculated DO profiles, using the BML approach (e.g., Figs. 3b and 3f), had RMS error e_{DO} < 5.3 mgL^{-1} (Figs. 3d and 3h). The Fickian sub-model improved DO prediction below the surface mixed layer (Figs. 3b and 3f). Instead of constant DO in the bottom boundary, the diffusive Fickian model reproduced the continuous decrease in DO concentration toward the sediments, and consequently had lower prediction error close to the bed (e_{DO} decreased from 3.6 mgL^{-1} to 2.6 mgL^{-1} at 30 m in Fig. 3d). This was due to the BML model was developed for central Lake Erie (Ivey & Patterson, 1984) which has strong near-bed seiche currents that drive a well-defined high shear and turbulent bottom boundary layer (Jabbari & Boegman, 2021; Jabbari et al., 2020; Valipour et al., 2015). There are not typically strong bottom currents in small Canadian Boreal lakes, (Ghane & Boegman, 2021; Oveisy & Boegman, 2014), which are characteristically sheltered, multi-basin, and deep. The mixed layer approach is, however, suitable in the surface layer for prediction of near-surface temperature and DO (Figs. 3a, 3b, 3e, and 3f), where the mixing depth is regulated by convection and the surface wind stress (Ghane & Boegman, 2021, 2023).

The Fickian model-simulated DO profiles were also closer to the observations above the hypolimnion (5 m<z<10 m and 7 m<z<13 m in Figs. 3b and 3f, respectively) and RMS error decreased through this region (e.g., e_{DO} at z=7 m decreased from 5.3 mgL^{-1} to 4.3 mgL^{-1} in Fig. 3d). The error was reduced further by including photosynthesis (e.g., e_{DO} decreased to 2 mgL^{-1} at z=7 m in Fig. 3d). As shown in Figs. 3b and 3f, the model reasonably predicted the observed sub-surface peak in photosynthetic oxygen production (~ z < 3 m) in both lakes (e_{DO} < 2 mgL^{-1}). This peak depends on the distribution of algal biomass and light attenuation (Munawar & Munawar, 1976; Patterson et al., 1985) and is a significant DO source, with production being modelled to provide ~90% of the net DO supply to Eagle Lake (Ghane & Boegman, 2023).

The model reproduced the characteristic seasonal changes in DO in both lakes (Figs. 2b and 2d). This included interannual variation in the effectiveness/completeness of spring and fall turnover events, which depend on interannual variation in local weather (Boegman et al., 2012; Ghane & Boegman, 2023; Molot et al., 1992). For example, there was strong turnover in the fall of 2011, in Eagle Lake, which resulted in a well oxygenated hypolimnion (~7 mgL^{-1}) until late summer of 2012 (Fig. 2d). Conversely, there was weak turnover during the fall of 2013 and the hypolimnion remained hypoxic from summer 2013 until fall 2014. These 1D model results are consistent with observations and simulations from a 3D model (Ghane & Boegman, 2023).

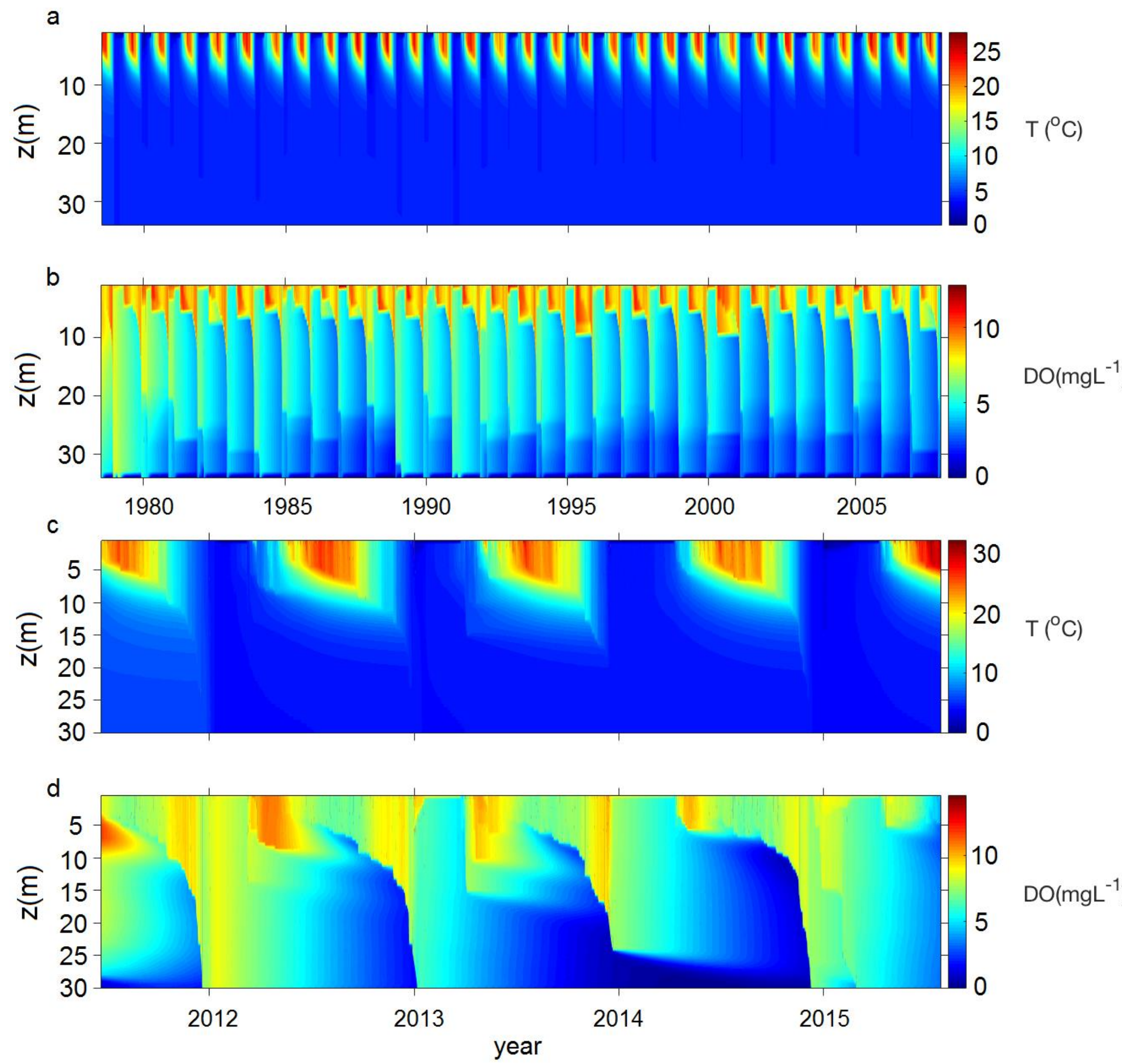

FIG. 2. Simulated time series of temperature (°C) (a and c) and dissolved oxygen (mgL^{-1}) (b and d) in Harp Lake (a and b) and Eagle Lake (c and d).

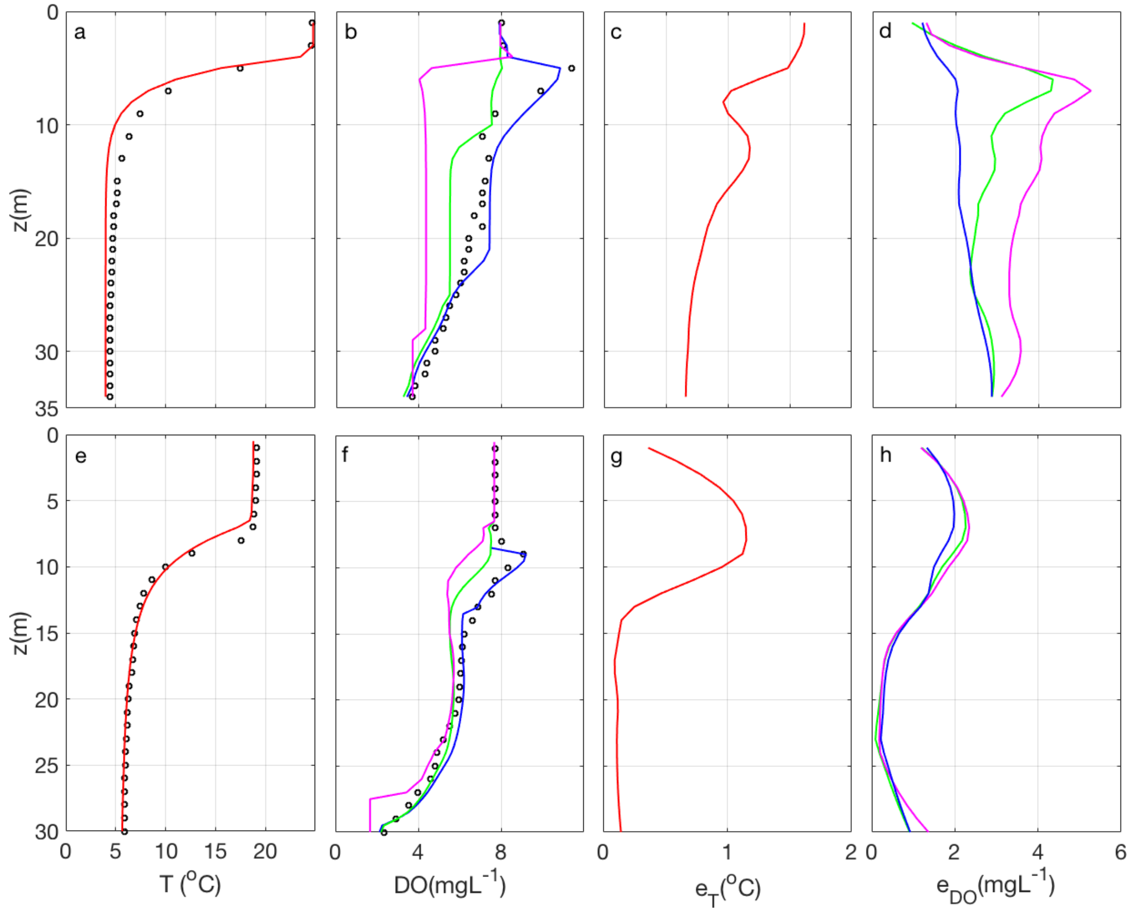

FIG. 3. Sample profiles of water temperature (°C) (a and e) and dissolved oxygen (mgL^{-1}) (b and f) from observations and various model results and RMS error for temperature (c and g) and dissolved oxygen (d and h) for Harp Lake (a, b, c, and d; a and b are on 22 Jul. 1991) and Eagle Lake (e, f, g, and h; e and f are on 22 Sep. 2011). In a, b, e, and f observations are open black circles. Colors in d and h are consistent with those in b and f; magenta: model using BML approach and constant HOD; green: model with Fickian flux sub-model and constant HOD, and blue: model with Fickian flux sub-model and photosynthesis modelling. RMS errors are calculated form 485 and 20 profiles of water temperature and dissolved oxygen all around the year in Harp Lake and Eagle Lake, respectively.

Table 1: Range of values used in model calibration and final value chosen, based on minimizing temperature and DO RMS error.

Parameter	Test range	Final value	Reference
Light extinction coefficient (m^{-1})	0.1-0.9	0.3 Eagle Lake, 0.5 Harp Lake	Ghane and Boegman (2023), MacKay (2012)
Hypolimnetic oxygen demand (HOD, $gm^{-3}d^{-1}$)	0.01-0.2	0.08 Eagle Lake, 0.03 Harp Lake	(Nakhaei et al., 2021), Bouffard et al. (2013)
Respiration rate (mg O_2 (mg Chl *a*)$^{-1}$ h^{-1}	0.05-5	1.8 and 0.2 in the upper and bottom mixed layers, respectively, for both lakes	Ganf (1974), Gibson 1975, Patterson et al. (1985)
α and β parameters (mg O_2 (mg Chl *a*)$^{-1}$ h^{-1} (Wm^{-2})$^{-1}$, Eq. 3)	0.05-10	0.1 and 4.2, respectively, for both lakes	Platt et al. (1980), Patterson et al. (1985)

Changes in GCM simulated climate from 1978 -2005 to 2071-2100

The GCM simulated mean summer (Aug. 15-Sep.15) air temperature, T_{air}, at Harp Lake increased significantly (p-value < 0.05) by 0.10 ± 0.07 (± standard error) °C year^{-1} during 1978- 2005 (Figure 4a). The mean summer T_{air} of 19.70 ± 2.89 °C during 1978-2005 (Fig. 4a) is also predicted to increase to 24.45 ± 2.04 °C, 25.22 ± 1.55 °C, and 28.43 ± 1.64 °C during 2071-2100, based on RCP 2.6, 4.5 and 8.5 projections, respectively (Fig. 4b). The GCM simulations also show that the average summer shortwave radiation will increase from 141.50 ± 10.81 Wm^{-2} during 1978-2005 (Fig. 4c) to 175.95 ± 16.28 Wm^{-2} during 2071-2100 (average of the three RCPs; Fig. 4d). The increases in air temperature and solar radiation are associated with decreased summer wind speed, from an average of 4.20 ± 0.31 ms^{-1} during 1978-2005 (Fig. 4e) to 3.34 ± 0.34 ms^{-1} during 2071-2100 (average of the three RCPs; Fig. 4f).

The RMS error, between the GCM predictions of seasonally averaged air temperature shortwave radiation and wind speed and the observed data, are smaller than the climate-induced changes (2.99 °C, 17.53 W m^{-2}, and 0.48 m s^{-1}). Warming of the surface layer and decreasing wind speeds will result in a shallower and warmer epilimnion, which has already been observed to be occurring in Canadian Boreal lakes (Nelligan et al., 2019). It remains unclear if this will result in lower hypolimnetic DO concentrations (because of DO depletion over a longer and stronger stratified period) or higher DO concentrations (because of a larger hypolimnetic volume from which DO depletion occurs).

Changes in simulated thermal structure from 1978 -2005 to 2071-2100

The atmospheric changes, predicted by the GCM, cause a thicker summer hypolimnion in Harp Lake (Figs. 5a vs 5c, S3a, and S3c) attributed to the warmer epilimnion and lower wind speeds (Fig. 4e vs 4f). The mean annual depth of the top of the hypolimnion (i.e., from the free surface to the top of hypolimnion below the metalimnion where the temperature gradient is < 1 °Cm^{-1}; D_H) at the end-of-summer (15 Aug. - 15 Sep.) is predicted to rise from 10.8 ± 1.07 m during 1978-2005 (Fig. 6a) to 9.0 ± 0.33 m during 2071-2100 (average of the three RCPs; Fig. 6b) representing an increase in hypolimnetic volume. The RMS errors in modelled D_H were 1.28 m and 0.54 m when using GCM and observed meteorological forcing, respectively, showing our lack of downscaling results in an additional ~0.74 m error in prediction of D_H.

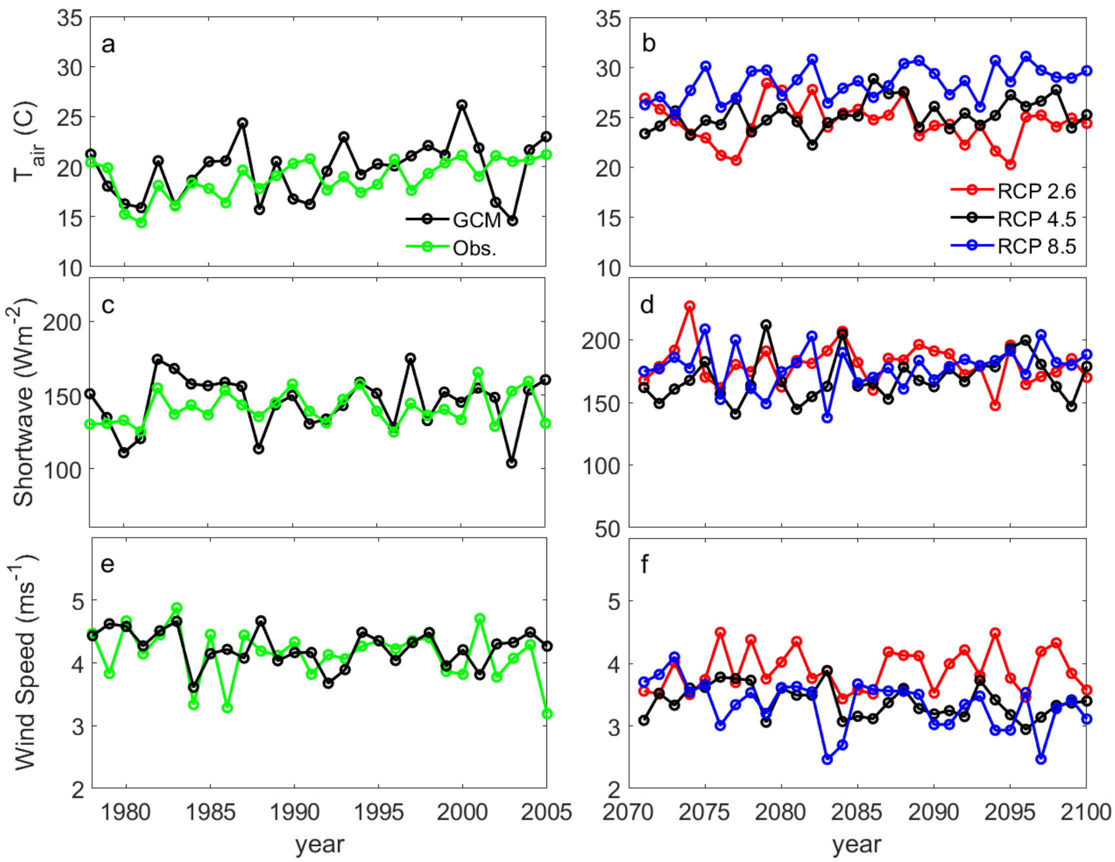

FIG. 4. Harp Lake end-of-summer (15 August-15 September) averaged air temperature (a and b), shortwave radiation (c and d), and wind speed (e and f) based on historical (a, c, and e; observed in green and GCM is black) and future (b, d, and f) GCM simulations (RCP 2.6, red; 4.5, black; 8.5, blue).

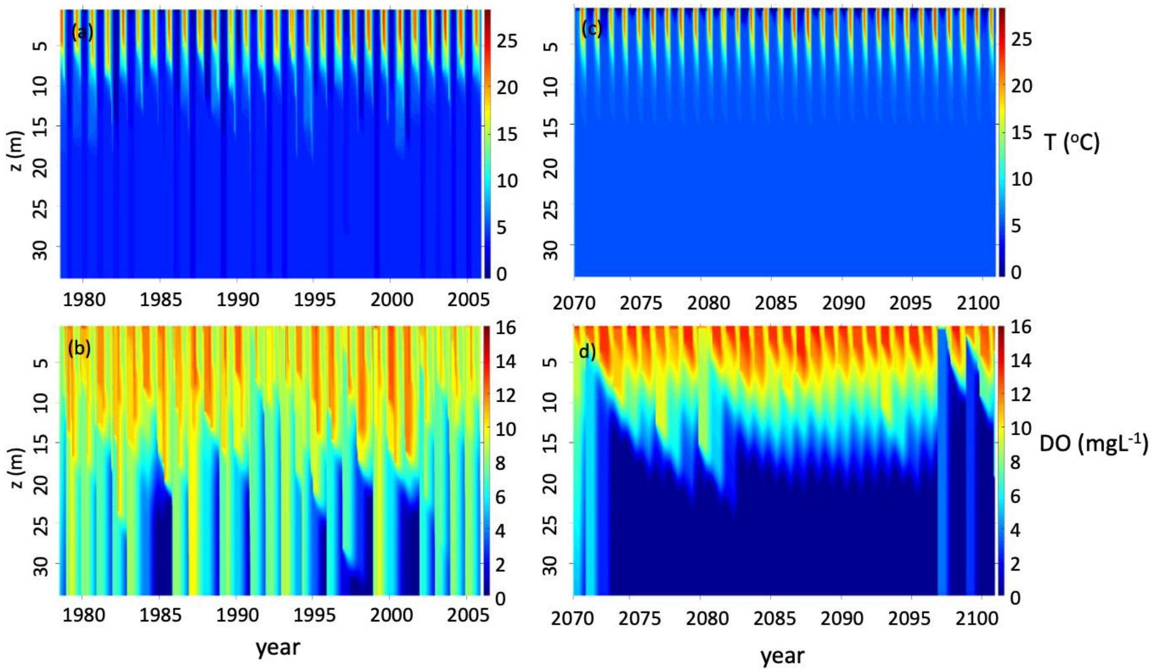

FIG. 5. Harp Lake, time series of historical (a and b) and future prediction (c and d; RCP 4.5) of water temperature (*T*; a and b) and dissolved oxygen (DO; c and d).

Changes in simulated DO from 1978 -2005 to 2071-2100

The mean volume-weighted hypolimnetic oxygen (VWHO) concentrations at the end-of-summer (15 Aug.-15 Sep. average) in Harp Lake showed a non-significant ($p > 0.05$; Table S1) decreasing trend of ~0.02 $mgL^{-1}y^{-1}$ during 1978-2007 (Fig. 6c) in our observations, the observations by Quinlan et al. (2005) and the model when forced by observed and by GCM meteorological data. The simulated VWHO were typically within $\pm$2 mg L^{-1} of the observed values and the RMS error were 1.14 mg L^{-1} (GCM forcing) and 1.09 mg L^{-1} (observed forcing), showing the error due to neglecting downscaling to be ~0.05 mg L^{-1}. This is much less than the up to 3 mg L^{-1} RMS error in simulation of observed DO profiles (Fig. 3) and the 1.06 mg L^{-1} RMS difference between our VWHO observations and those by Quinlan et al. (2005)(Fig. 6c). The VWHO decreased from a mean value of 6.27 $\pm$ 1.09 mg L^{-1} during 1978-2005 (from GCM, Fig. 6c) to 1.36 $\pm$ 0.86 mg L^{-1} during 2071-2100 (average of 3 RCPs; Fig. 6d). This was simulated to occur, despite an increase in the future hypolimnetic volume (Fig. 5b vs 5d, S3b and S3d), which would accommodate a larger DO reservoir to buffer DO depletion (Nakhaei et al., 2021).

During this time, temperature-induced changes in volume-weighted hypolimnetic reseparation (i.e., biological DO sinks), and photosynthesis (i.e., biological source of DO) were negligible (~10^{-4} mg $L^{-1}h^{-1}$ and ~10^{-6} mg $L^{-1}h^{-1}$, respectively; Figs. 6e and 6f). Moreover, the sediment oxygen demand approached zero in most years (Figs. 6e and 6f) due to the lack of an oxygen gradient from the hypolimnion to the sediments (equation 5), as a hypoxic hypolimnion was predicted in many future years (Figs. S3b, 5d and S3d).

Periodic increases in the future bottom DO concentration during the fall and spring (e.g., years 2072, 2074, 2078, 2095, 2097 in Fig. 7b) can be attributed to seasonal lake turnovers, where the surface mixed layer depth h_s penetrated deep into the hypolimnion. The models predicted less frequent seasonal turnovers that led to reduced bottom re-oxygenation in the future (e.g., 5 events during 2071-2100; Fig. 7b vs. 25 events during 1978-2005; Fig. 7a). The number of future reoxygenation events during turnover decreased with an increase in future emissions (5, 4 and 2 deep mixing events for RCP 2.6, 4.5 and 8.5, respectively, neglecting model spin-up). Apart from these occasional years, when the surface mixed layer extends to the bottom during turnover, the model predicts a hypoxic hypolimnion in most of the future years, e.g., 23 hypoxic summertime years during 2071-2100 based on RCP 2.6 (Fig. 7a). These results, when combined with those in Fig. 6e-f, show that physical processes (for example, less frequent complete seasonal mixing), rather than biological processes (Bouffard et al., 2013; Ladwig et al., 2021; Nakhaei et al., 2021) are the first order contributors to climate driven hypolimnetic hypoxia in the future. As a result, much longer periods of hypoxia (e.g., 16 years from 2080-2095, based on RCP 2.6; Fig. 7a) are predicted for the future. Conversely, episodic hypoxia only occurred in limited years in the past, e.g., 9 episodic hypoxic summers during 1978-2005; Fig. 7a.

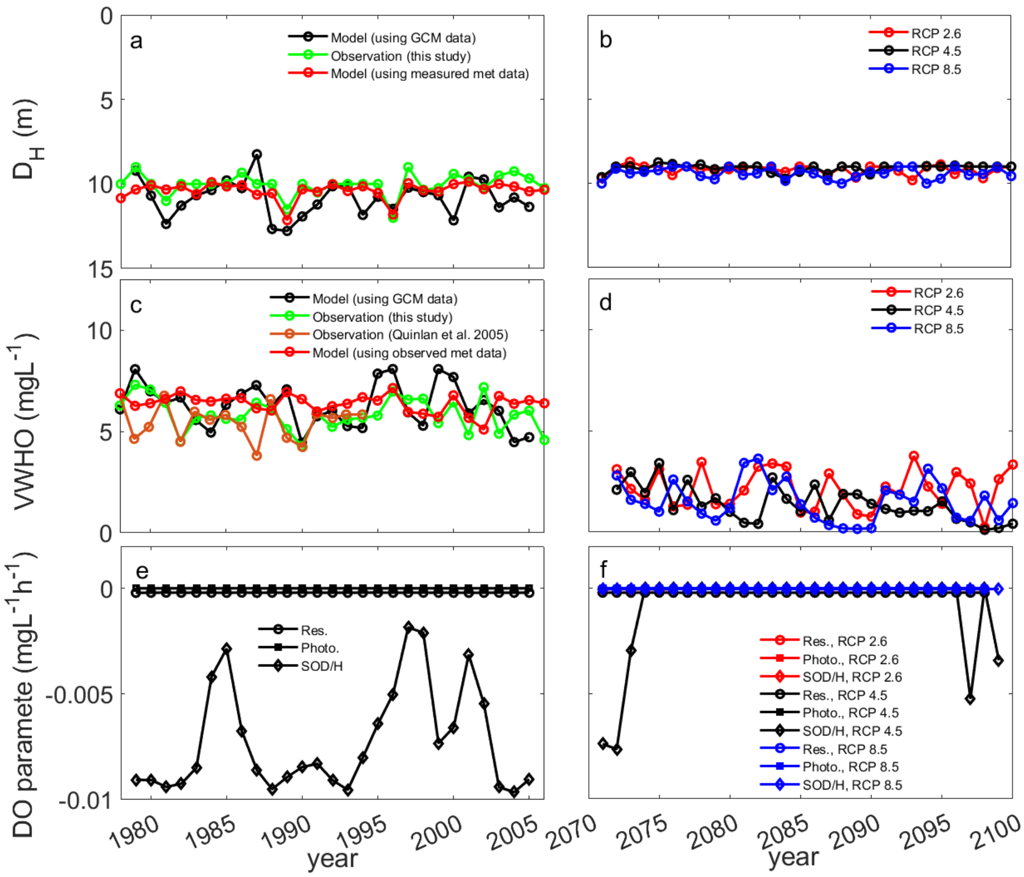

FIG. 6. In Harp Lake, end-of-summer (15 August-15 September) annual average of the depth of hypolimnion (D_H; a and b), volume-weighted hypolimnetic oxygen (VWHO; c and d), volume-weighted hypolimnetic reseparation (circle; e and f), volume-weighted hypolimnetic photosynthesis (square; e and f) and the rate of sediment oxygen demand normalized by the thickness of hypolimnion (diamond; e and f) based on historical GCM (black in a, c, and e) and future GCM simulations (b, d, and f) (RCP 2.6, red; RCP 4.5, black; RCP 8.5, blue). Green lines in a and c represent calculations from observation data in this study and orange line in c is from the field measurements from Quinlan et al. (2005). Red lines in a and c are from model using measured meteorological data.

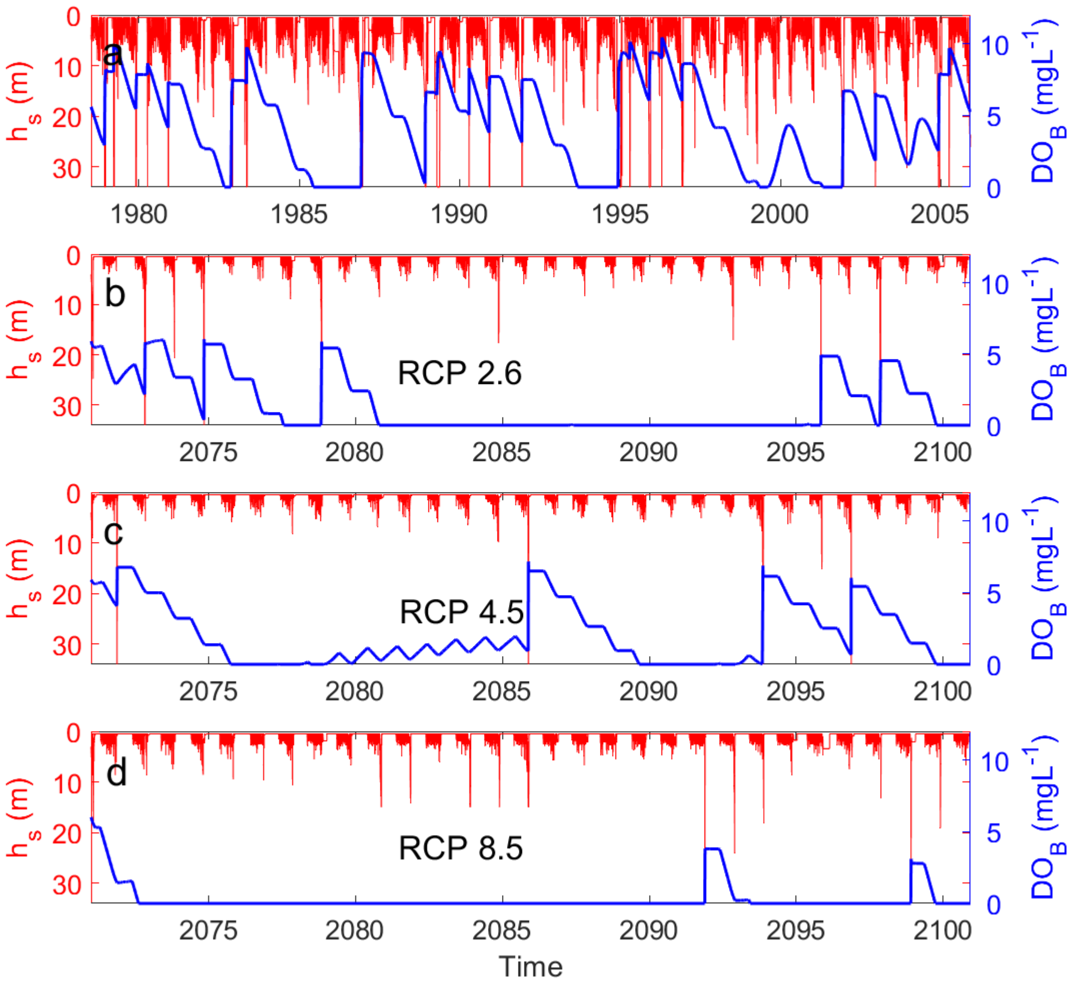

FIG. 7. In Harp Lake, surface mixed layer depth (h_s; red) and the bottom dissolved oxygen concentration (DO_B; 5 m above the bed; blue) from the historical (a) and future (RCP 2.6 (b), 4.5 (c), and 8.5 (d)) climate forcing data from global climate model (GCM).

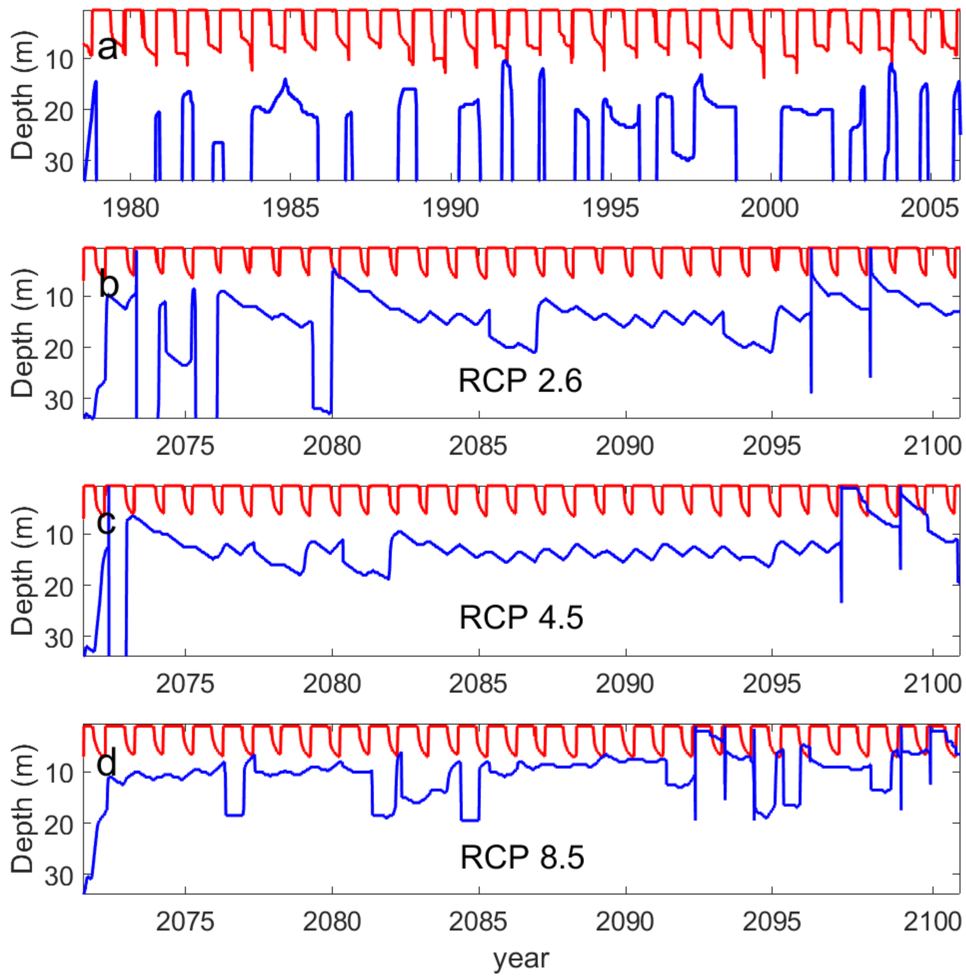

FIG. 8. Lake trout habitat plots in Harp Lake: the depths of the 10°C isotherm (red) and 5 mg L^{-1} (blue) isopleth from the historical (a) and future (RCP 2.6 (b), 4.5 (c), and 8.5 (d)) climate forcing data from global climate model (GCM).

Discussion and conclusions

We developed a simple DO sub-model that was implemented into a one-dimensional bulk mixed-layer thermodynamic model for hindcasting and prediction of temperature and dissolved oxygen in two Canadian lake trout lakes. Using minimal model parameters, photosynthetic production and respiration were calculated as functions of light intensity, water temperature, and oxygen concentration at constant nutrient inputs. The model predicted temperature and DO profiles with root-mean-square error <1.5 °C and <3 mgL^{-1}, respectively. These errors are consistent with those in the literature for other 1D lake models of temperature (Bruce et al., 2018; Oveisy & Boegman, 2014; Perroud et al., 2009) and oxygen (Bolkhari et al., 2022; Ladwig et al., 2021; Snortheim et al., 2017).

Prediction of oxygen concentrations in lake ecosystems has crucial management implications for understanding habitat availability for vulnerable aquatic species under stress from climate change (Nelligan et al., 2019). Lake trout are a cold water species that prefer water temperatures <~10 °C and DO concentrations >~6 mg L^{-1} (Dillon et al., 2003). Therefore, they often inhabit the strata of water column below the warm surface layer and above the deoxygenated hypolimnion. With climate warming, there is potential for increased hypoxia, which will stress the lake trout habitat (Nelligan et al., 2019). Both Eagle Lake and Harp Lake have been classified as 'at capacity' by the Ontario Ministry of the Environment, Conservation and Parks, because their end-of-summer mean volume-weighted hypolimnetic DO concentration (VWHO) has been near or below the provincial standard (7 mg L^{-1}; (Evans, 2007)) for juvenile lake trout lake (Fig. 6c). Future climate predictions (2071-2100) for Harp Lake show an increase in the mean end-of-summer (15 Aug. - 15 Sep.) air temperature (Figs. 4a and 4b), which is consistent with predicted contiguous climate warming across Ontario during the next century (Wang et al., 2014) and historical warming of the water surface temperature in the Great Lakes (Huang et al., 2012; Jabbari et al., 2021). The future climate scenarios predict mean end-of-summer simulated VWHO <5 mg L^{-1} (Fig. 6d), well below lake trout habitat suitability. The decreased VWHO at the end-of-summer results from a reduction in the frequency of deep vertical mixing of DO during turnover events and will occur while changes to the contribution of biological sinks and sources of oxygen (i.e., respiration, photosynthesis, and sediment oxygen demand; Figs. 6e and 6f) remain negligible. Despite GCM predicted increases in air temperature of 4.8, 5.5 and 8.7 °C, between 1978-2005 and 2071-2100, under RCP 2.6, 4.5 and 8.5, respectively, the associated simulated differences between VWHO are minimal (2.1 ± 1.0, 1.4 ± 0.9 and 1.5 ± 1.0 mg L^{-1}; mean ± standard deviation) in comparison to their difference from the 6.3 ± 1.1 GCM-simulated value over 1978-2005. This shows that a fundamental shift in lake mixing behavior is occurring for RCP 2.6, with the additional warming for RCP 4.5 and 8.5 having a minimal additional impact in further reducing VWHO.

Several water quality and ecological consequences are associated with these alternations in lake mixing regime including stress to vulnerable fish species (Arend et al., 2011). For example, lake trout are typically limited within the water column to regions with high DO concentration and low water temperature. Earlier analyses used the concepts of optimal and usable temperature and DO as habitat boundaries. For lake trout, the water strata should have a temperature <10 ºC and DO > 6 mg L^{-1} to be considered optimal habitat (MOE & MNR, 1986); similarly, water with temperature between 10 and 15 ºC and DO between 4 and 6 mg L^{-1} is defined as usable habitat (Evans et al., 1991). While this approach provides readily interpreted habitat figures, it is not a weighted average measure and so does not account for changes in the quantity of habitat, unlike the VWHO criterion which does not explicitly account for temperature, but rather considers the hypolimnion temperature to be optimal.

We compare the depth of water column habitat, H_{Hab}, between the simulated 10 °C isotherm and 5 mg L^{-1} isopleth, as an indicator of lake trout habitat with historical (Fig. 8a) and future (Fig. 8b-d) climate forcing data. The figures show that the habitat region for lake trout will decrease significantly from ~2 years with no suitable habitat during late summer (1978 -2005), to nearly all years having no suitable habitat from 2090 onwards under RCP 8.5. On average, H_{Hab} on 15 Sept., the latest recommended date to monitor end-of-summer VWHO in an Ontario lake trout lake (MOE et al., 2010), declines with increasing greenhouse gas emissions, from 17±8.5 m (mean ± standard deviation) during 1978-2005 to 2±2.6 m during 2071-2100 (Fig. 9). These results show that climate change can drastically impact the habitat for lake trout which are a keystone species in many Canadian Boreal aquatic ecosystems (Minns et al., 2008).

A reduction in the frequency of deep mixing during fall turnover is predicted in the future for all RCPs (Fig. 7b to 7d). These mixing events are, critically, the only time of year when there is sufficient wind energy for dimictic lakes to mix vertically (Boegman, 2020). The reduced mixing results from a greater temperature difference between the surface and the bottom of the metalimnion. For example, Fig. S4a shows greater resistance to water column mixing for a representative future year (2090; RCP 4.5) than a year in the past (1985). This simulated behavior is consistent with observations, in temperate lakes, of lengthening (Stainsby et al., 2011) and strengthening (Nelligan et al., 2019) seasonal summer stratification causing a reduction in deep water DO (Bukaveckas et al., 2023). The systemic reduction in the depth of seasonal dimictic mixing during turnover events (Fig. 7), suggests small Canadian Boreal lakes will adopt the mixing characteristics of lakes in Europe (e.g., Lake Geneva (Schwefel et al., 2017)) and Japan (e.g., Lake Ikeda (Boehrer et al., 2009)), that only fully mix in exceptional years, when the extended surface mixed layer oxygenates the bottom of the lake; the hypolimnia of these lakes otherwise remains anoxic. A key driver of this change in lake mixing behavior (Woolway et al., 2019) is the climate driven increase in lake surface temperature (Fig. 4), which strengthens and prolongs summer stratification (Fig. S4a), reducing the strength of convective turnover. Our prediction of a fundamental climate-induced reduction lake mixing is consistent with the modelling work by Woolway and Merchant (2019), who applied FLake, coupled to the ISIMIP2b climate projections, to predict worldwide climate-induced changes in lake mixing. In the Harp Lake region, they predicted lakes to shift from dimictic to warm monomictic (mixes once a year) or warm monomictic to meromictic (does not mix), consistent with our results.

Given that lake mixing classifications do not account for the depth of mixing, and that the depth of mixing varies interannually in Harp Lake, with a profound impact on the bottom water DO concentration (Fig. 7), we are reluctant to classify how the mixing regime is expected to change in the future. Nonetheless, according to Wetzel (2023), the predicted future of Harp Lake fits the definition of oligomictic, undergoing ‘full circulation of the water column in intermittent years’ and which, ‘occurs among lakes of small surface area and moderate depth that are sheltered, especially in continental regions that experience long winters’. However, in earlier definitions (Wetzel, 2001), both warm monomictic and oligomictic lakes are ‘not ice covered’. In our simulations, Harp Lake remained ice-covered in future winters (Fig. S4b,c). There is evidence that deep convection is already being inhibited by climate-induced warning in Lake Zurich (Yankova et al., 2017) and this has been altering plankton dynamics over the past ~10 years (Posch et al., 2012).

In this study, we considered two moderately deep lakes (~30 m). Future increased resistance to water column mixing will also have profound implications for shallower systems. For example, we expect more frequent and longer development of episodic hypoxic events at the sediment-water interface in shallow (Bukaveckas et al., 2023) and polymictic (Jabbari et al., 2019; Loewen et al., 2007) systems and above the hypolimnion in thermally stratified systems (Stow et al., 2023). This has been observed to relegate fish to surface waters and increase sediment release of phosphate, ammonia and methane (Søndergaard et al., 2023).

Our data also show some significant trends ($p < 0.05$) over the past several decades (Table S1). There was a statistically significant increase of 0.10 °C yr^{-1} in the observed mean Aug. 15-Sep. 15 air temperature during 1978-2007. The analogous GCM simulated air temperature had the same increase, but the trend was not significant, likely due to strong inter-annual variability (Fig. 4a). There were no significant corresponding observed or GCM modelled trends in thermocline depth. We also did not model (Fig 6c, 1978-2005) or observe (Fig. 6c, 1978-2005 and1976-1994 from Quinlan et al. (2005)) significant trends in the Aug. 15-Sep. 15 average VWHO. However, Nelligan et al. (2019) observed a significant trend of increasing Sep. 15 VWHO = 0.034 mg $L^{-1}y^{-1}$ during 1978-2016 in Harp Lake (Table S1), which they noted are counter to the expected influence of warming on lake oxygen (Foley et al., 2012). They argued this difference resulted from trends in primary production, which we do not explicitly model.

A conceptual limitation of our modelling framework is the usage of a 1D model that does not capture the influence of sidearm convection on lake turnover. However, a 3D modelling study of Eagle Lake (Ghane & Boegman, 2021, 2023) revealed that side-arm convection contributed less than 5% of the vertical mass flux during turnover with the remainder being driven by mid-basin convection penetrative convection, which is well parameterized in a 1D mixed-layer model.

In conclusion, the mean summer air temperature in the Harp Lake region has been predicted to increase by 4.8, 5.5 and 8.7 °C from 1978-2005 to 2071-2100, based on RCP 2.6, 4.5 and 8.5 projections. We have modelled this climate forcing to reduce the mean end-of-summer VWHO from 6.3 mgL^{-1} during 1978-2005 to 1.4 mgL^{-1} during 2071-2100 (average of 3 RCPs), well below the provincial threshold of 7 mgL^{-1} for a lake trout lake. Our model predicts that climate warming reduces the effectiveness/completeness of the spring and fall turnover events which replenish DO to the hypoxic hypolimnion. As a result, the average amount of lake trout habitat, on 15 Sept., will be reduced from ~17 m during 1978-2005 to ~8, ~6, or ~2 m for RCP 2.6, 4.5 and 8.5, respectively, during 2071-2100. These changes, as modelled in Harp Lake, indicate that climate change will have significant impacts on lake trout colonization ranges (Campana et al., 2020), with important implications for the future management of cold-water fish populations.

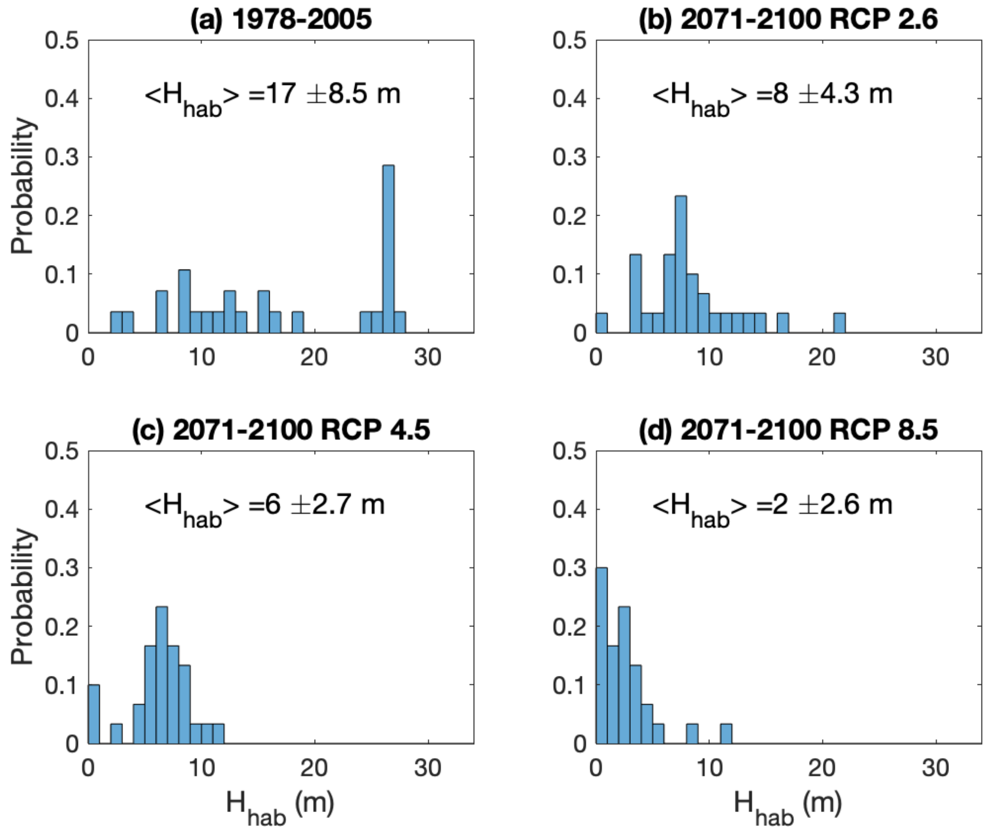

FIG. 9: Simulated probability distribution of H_{Hab} on 15 Sept. during (a) 1978-2005; (b) 2071-2100 under RCP 2.6; (c) 2071-2100 under RCP 4.5; and (d) 2071-2100 under RCP 8.5. The angled parentheses denote the mean value ± the standard deviation.

Acknowledgements

We thank Murray MacKay for assistance with implementing the DO sub-model into the CSLM and for providing the GCM forcing data. We thank Andrew Paterson for providing the Harp Lake field data. This project was funded by an NSERC Strategic Projects grant to John Smol (PI), LB and LM.

Conflict of interest

All authors declare that they have no conflicts of interest.

Data Availability

All the data and codes in this study can be obtained from the corresponding author upon request.

References

Arend, K., Beletsky, D., DePinto, J. V., Ludsin, S. A., Roberts, J. J., Rucinski, D. K., et al. (2011). Seasonal and interannual effects of hypoxia on fish habitat quality in central Lake Erie. *Freshwater Biology, 56*(2), 366-383. https://onlinelibrary.wiley.com/doi/abs/10.1111/j.1365-2427.2010.02504.x

Boegman, L. (2020). Hydrodynamics of Lakes. In P. Maurice (Ed.), *Encyclopedia of Water: Science, Technology, and Society* (pp. 11): Wiley.

Boegman, L., Shkvorets, I., & Johnson, F. (2012). *Hypoxia and turnover in a small ice-covered temperate lake.* Paper presented at the 21st IAHR International Symposium on Ice, Dalian, China.

Boehrer, B., Fukuyama, R., Chikita, K., & Kikukawa, H. (2009). Deep water stratification in deep caldera lakes Ikeda, Towada, Tazawa, Kuttara, Toya and Shikotsu. *Limnology, 10*(1), 17-24. https://doi.org/10.1007/s10201-008-0257-1

Bolkhari, H., Boegman, L., & Smith, R. E. H. (2022). Simulated impacts of climate change on Lake Simcoe water quality. *Inland Waters, 12*(2), 215-231. https://doi.org/10.1080/20442041.2021.1969190

Bouffard, D., Ackerman, J. D., & Boegman, L. (2013). Factors affecting the development and dynamics of hypoxia in a large shallow stratified lake: hourly to seasonal patterns. *Water Resources Research, 49*(5), 2380-2394.

Bruce, L. C., Frassl, M. A., Arhonditsis, G. B., Gal, G., Hamilton, D. P., Hanson, P. C., et al. (2018). A multi-lake comparative analysis of the General Lake Model (GLM): Stress-testing across a global observatory network. *Environ. Model. Softw., 102*, 274-291.

Bukaveckas, P. A., Buikema, L., & Stewart, C. (2023). Effects of climate change and variability on thermal regime and dissolved oxygen resources of oligotrophic lakes in the Adirondack Mountain region. *Aquatic Sciences, 86*(1), 9. https://doi.org/10.1007/s00027-023-01021-2

Campana, S. E., Casselman, J. M., Jones, C. M., Black, G., Barker, O., Evans, M., et al. (2020). Arctic freshwater fish productivity and colonization increase with climate warming. *Nature Climate Change, 10*(5), 428-433. https://doi.org/10.1038/s41558-020-0744-x

Dillon, P. J., Clark, B. J., Molot, L. A., & Evans, H. E. (2003). Predicting the location of optimal habitat boundaries for lake trout (Salvelinus namaycush) in Canadian Shield lakes. *Canadian Journal of Fisheries and Aquatic Sciences, 60*(8), 959-970. https://cdnsciencepub.com/doi/abs/10.1139/f03-082

Evans, D. O. (2007). Effects of hypoxia on scope-for-activity and power capacity of lake trout (Salvelinus namaycush). *Canadian Journal of Fisheries and Aquatic Sciences, 64*(2), 345-361. https://cdnsciencepub.com/doi/abs/10.1139/f07-007

Evans, D. O., Casselman, J. M., & Willox, C. C. (1991). *Effects of exploitation, loss of nursery habitat, and stocking on the dynamics and productivity of lake trout populations in Ontario lakes: Lake trout synthesis, response to stress working group*: Ontario Ministry of Natural Resources.

Farmer, D. M., & Carmack, E. C. (1981). Wind Mixing and Restratification in a Lake near the Temperature of Maximum Density. *Journal of Physical Oceanography, 11*(11), 1516-1533. https://journals.ametsoc.org/view/journals/phoc/11/11/1520-0485_1981_011_1516_wmaria_2_0_co_2.xml

Ficke, A. D., Myrick, C. A., & Hansen, L. J. (2007). Potential impacts of global climate change on freshwater fisheries. *Reviews in Fish Biology and Fisheries, 17*(4), 581-613. https://doi.org/10.1007/s11160-007-9059-5

Fischer, H., List, E., Koh, R., Imberger, J., & Brooks, N. (1979). *Mixing in Inland and Coastal Waters*. New York: Academic Press.

Foley, B., Jones, I. D., Maberly, S. C., & Rippey, B. (2012). Long-term changes in oxygen depletion in a small temperate lake: effects of climate change and eutrophication. *Freshwater Biology, 57*(2), 278-289. https://onlinelibrary.wiley.com/doi/abs/10.1111/j.1365-2427.2011.02662.x

Ganf, G. G. (1974). Rates of oxygen uptake by the planktonic community of a shallow equatorial lake (Lake George, Uganda). *Oecologia, 15*(1), 17-32. https://doi.org/10.1007/BF00345226

Garnaud, C., MacKay, M., & Fortin, V. (2022). A One-Dimensional Lake Model in ECCC's Land Surface Prediction System. *Journal of Advances in Modeling Earth Systems, 14*(2), e2021MS002861. https://agupubs.onlinelibrary.wiley.com/doi/abs/10.1029/2021MS002861

Ghane, A., & Boegman, L. (2021). Turnover in a small Canadian shield lake. *Limnology and Oceanography, 66*(9), 3356-3373. https://aslopubs.onlinelibrary.wiley.com/doi/abs/10.1002/lno.11884

Ghane, A., & Boegman, L. (2023). The dissolved oxygen budget of a small Canadian Shield lake during winter. *Limnology and Oceanography, 68*(1), 265-283. https://aslopubs.onlinelibrary.wiley.com/doi/abs/10.1002/lno.12265

Gibson, C. E. (1975). A Field and Laboratory Study of Oxygen Uptake by Planktonic Blue-Green Algae. *Journal of Ecology, 63*(3), 867-879. http://www.jstor.org/stable/2258607

Guzzo, M. M., & Blanchfield, P. J. (2017). Climate change alters the quantity and phenology of habitat for lake trout (Salvelinus namaycush) in small Boreal Shield lakes. *Canadian Journal of Fisheries and Aquatic Sciences, 74*(6), 871-884. https://cdnsciencepub.com/doi/abs/10.1139/cjfas-2016-0190

Hamilton, D. P., & Schladow, S. G. (1997). Prediction of water quality in lakes and reservoirs. Part I—Model description. *Ecol. Modell., 96*(1-3), 91-110.

Huang, A., Rao, Y. R., & Zhang, W. (2012). On recent trends in atmospheric and limnological variables in Lake Ontario. *Journal of Climate, 25*(17), 5807-5816. https://journals.ametsoc.org/view/journals/clim/25/17/jcli-d-11-00495.1.xml

Hurtado, D. C., Boegman, L., Hofmann, H., & Jabbari, A. (2023). Prediction of future Alaskan lake methane emissions using a small-lake model coupled to a regional climate model. *Authorea Preprints*.

Imberger, J. (1985). The diurnal mixed layer. *Limnology & Oceanography, 30*(4), 737-770.

Ivey, G. N., & Patterson, J. C. (1984). A model of the vertical mixing in Lake Erie in summer. *Limnology and Oceanography, 29*(3), 553-563. https://aslopubs.onlinelibrary.wiley.com/doi/abs/10.4319/lo.1984.29.3.0553

Jabbari, A., Ackerman, J. D., Boegman, L., & Zhao, Y. (2019). Episodic hypoxia in the western basin of Lake Erie. *Limnology and Oceanography, 64*(5), 2220-2236. https://aslopubs.onlinelibrary.wiley.com/doi/abs/10.1002/lno.11180

Jabbari, A., Ackerman, J. D., Boegman, L., & Zhao, Y. (2021). Increases in Great Lake winds and extreme events facilitate interbasin coupling and reduce water quality in Lake Erie. *Scientific reports, 11*(1), 5733. https://doi.org/10.1038/s41598-021-84961-9

Jabbari, A., & Boegman, L. (2021). Parameterization of oscillating boundary layers in lakes and coastal oceans. *Ocean Modelling, 160*, 101780. https://www.sciencedirect.com/science/article/pii/S1463500321000305

Jabbari, A., Boegman, L., Valipour, R., Wain, D., & Bouffard, D. (2020). Dissipation of turbulent kinetic energy in the oscillating bottom boundary layer of a large shallow lake. *Journal of Atmospheric and Oceanic Technology, 37*(3), 517-531.

Jankowski, T., Livingstone, D. M., Bührer, H., Forster, R., & Niederhauser, P. (2006). Consequences of the 2003 European heat wave for lake temperature profiles, thermal stability, and hypolimnetic oxygen depletion: Implications for a warmer world. *Limnology and Oceanography, 51*(2), 815-819. https://aslopubs.onlinelibrary.wiley.com/doi/abs/10.4319/lo.2006.51.2.0815

Ladwig, R., Hanson, P. C., Dugan, H. A., Carey, C. C., Zhang, Y., Shu, L., et al. (2021). Lake thermal structure drives interannual variability in summer anoxia dynamics in a eutrophic lake over 37 years. *Hydrol. Earth Syst. Sci., 25*(2), 1009-1032. https://hess.copernicus.org/articles/25/1009/2021/

Loewen, M. R., Ackerman, J. D., & Hamblin, P. F. (2007). Environmental implications of stratification and turbulent mixing in a shallow lake basin. *Canadian Journal of Fisheries and Aquatic Sciences, 64*(1), 43-57.

MacKay. (2012). A process-oriented small lake scheme for coupled climate modeling applications. *Journal of Hydrometeorology, 13*(6), 1911-1924. https://journals.ametsoc.org/view/journals/hydr/13/6/jhm-d-11-0116_1.xml

MacKay, Neale, P. J., Arp, C. D., De Senerpont Domis, L. N., Fang, X., Gal, G., et al. (2009). Modeling lakes and reservoirs in the climate system. *Limnology and Oceanography, 54*(6part2), 2315-2329. https://aslopubs.onlinelibrary.wiley.com/doi/abs/10.4319/lo.2009.54.6_part_2.2315

MacKay, Verseghy, D. L., Fortin, V., & Rennie, M. D. (2017). Wintertime Simulations of a Boreal Lake with the Canadian Small Lake Model. *Journal of Hydrometeorology, 18*(8), 2143-2160. https://journals.ametsoc.org/view/journals/hydr/18/8/jhm-d-16-0268_1.xml

Minns, C. K., Moore, J. E., Shuter, B. J., & Mandrak, N. E. (2008). A preliminary national analysis of some key characteristics of Canadian lakes. *Canadian Journal of Fisheries and Aquatic Sciences, 65*(8), 1763-1778. https://cdnsciencepub.com/doi/abs/10.1139/F08-110

MOE, & MNR. (1986). *Inland lake trout management in eastern Ontario* (MNR 52013). Retrieved from Peterborough, ON:

MOE, MNRF, & MMAH. (2010). *Lakeshore Capacity Assessment Handbook: Protecting Water Quality in Inland Lakes.* Retrieved from Ontario:

Molot, L. A., Dillon, P. J., Clark, B. J., & Neary, B. P. (1992). Predicting End-of-Summer Oxygen Profiles in Stratified Lakes. *Canadian Journal of Fisheries and Aquatic Sciences, 49*(11), 2363-2372. https://cdnsciencepub.com/doi/abs/10.1139/f92-260

Munawar, M., & Munawar, I. F. (1976). A lakewide study of phytoplankton biomass and its species composition in Lake Erie, April–December 1970. *Journal of the Fisheries Board of Canada, 33*(3), 581-600.

Nakhaei, N., Ackerman, J. D., Bouffard, D., Rao, Y. R., & Boegman, L. (2021). Empirical modeling of hypolimnion and sediment oxygen demand in temperate Canadian lakes. *Inland Waters*, 1-17. https://doi.org/10.1080/20442041.2021.1880244

Nakhaei, N., Boegman, L., & Bouffard, D. (2016). *Measurement of vertical oxygen flux in lakes from microstructure casts*. Paper presented at the VIIIth International Symposium on Stratified Flows, San Diego, CA. https://escholarship.org/uc/item/12p56378

Nelligan, C., Jeziorski, A., Rühland, K. M., Paterson, A. M., & Smol, J. P. (2016). Managing lake trout lakes in a warming world: a paleolimnological assessment of nutrients and lake production at three Ontario sites. *Lake and Reservoir Management, 32*(4), 315-328. https://doi.org/10.1080/10402381.2016.1203844

Nelligan, C., Jeziorski, A., Rühland, K. M., Paterson, A. M., & Smol, J. P. (2019). Long-term trends in hypolimnetic volumes and dissolved oxygen concentrations in Boreal Shield lakes of south-central Ontario, Canada. *Canadian Journal of Fisheries and Aquatic Sciences, 76*(12), 2315-2325. https://cdnsciencepub.com/doi/abs/10.1139/cjfas-2018-0278

Oveisy, A., & Boegman, L. (2014). One-dimensional simulation of lake and ice dynamics during winter. *Journal of Limnology, 73*(3). https://www.jlimnol.it/index.php/jlimnol/article/view/jlimnol.2014.903

Patterson, J. C., Alanson, B. R., & Ivey, G. N. (1985). A dissolved oxygen budget model for Lake Erie in summer. *Freshwater Biology, 15*(6), 683-694. https://onlinelibrary.wiley.com/doi/abs/10.1111/j.1365-2427.1985.tb00242.x

Perroud, M., Goyette, S., Martynov, A., Beniston, M., & Annevillec, O. (2009). Simulation of multiannual thermal profiles in deep Lake Geneva: A comparison of one-dimensional lake models. *Limnology and Oceanography, 54*(5), 1574-1594. https://aslopubs.onlinelibrary.wiley.com/doi/abs/10.4319/lo.2009.54.5.1574

Platt, T., Gallegos, C., & Harrison, W. (1980). Photoinhibition of photosynthesis in natural assemblages of marine phytoplankton. *Journal of Marine Research, 38*(4).

Posch, T., Köster, O., Salcher, M. M., & Pernthaler, J. (2012). Harmful filamentous cyanobacteria favoured by reduced water turnover with lake warming. *Nature Climate Change, 2*(11), 809-813. https://doi.org/10.1038/nclimate1581

Quinlan, R., Douglas, M. S. V., & Smol, J. P. (2005). Food web changes in arctic ecosystems related to climate warming. *Global Change Biology, 11*(8), 1381-1386. https://onlinelibrary.wiley.com/doi/abs/10.1111/j.1365-2486.2005.00981.x

Robson, B. J., & Hamilton, D. P. (2004). Three-dimensional modelling of a Microcystis bloom event in the Swan River estuary, Western Australia. *Ecological modelling, 174*(1), 203-222. https://www.sciencedirect.com/science/article/pii/S0304380004000080

Schwefel, R., Gaudard, A., Wüest, A., & Bouffard, D. (2016). Effects of climate change on deepwater oxygen and winter mixing in a deep lake (Lake Geneva): Comparing observational findings and modeling. *Water Resources Research, 52*(11), 8811-8826. https://agupubs.onlinelibrary.wiley.com/doi/abs/10.1002/2016WR019194

Schwefel, R., Steinsberger, T., Bouffard, D., Bryant, L. D., Müller, B., & Wüest, A. (2017). Using small-scale measurements to estimate hypolimnetic oxygen depletion in a deep lake. *Limnology and Oceanography*.

Sharma, S., Jackson, D. A., & Minns, C. K. (2009). Quantifying the potential effects of climate change and the invasion of smallmouth bass on native lake trout populations across Canadian lakes. *Ecography, 32*(3), 517-525. https://onlinelibrary.wiley.com/doi/abs/10.1111/j.1600-0587.2008.05544.x

Smol, J. P. (2010). The power of the past: using sediments to track the effects of multiple stressors on lake ecosystems. *Freshwater Biology, 55*(s1), 43-59. https://onlinelibrary.wiley.com/doi/abs/10.1111/j.1365-2427.2009.02373.x
Snortheim, C. A., Hanson, P. C., McMahon, K. D., Read, J. S., Carey, C. C., & Dugan, H. A. (2017). Meteorological drivers of hypolimnetic anoxia in a eutrophic, north temperate lake. *Ecol. Modell., 343*, 39-53.
Søndergaard, M., Nielsen, A., Skov, C., Baktoft, H., Reitzel, K., Kragh, T., & Davidson, T. A. (2023). Temporarily and frequently occurring summer stratification and its effects on nutrient dynamics, greenhouse gas emission and fish habitat use: case study from Lake Ormstrup (Denmark). *Hydrobiologia, 850*(1), 65-79. https://doi.org/10.1007/s10750-022-05039-9
Spigel, R. H., Imberger, J., & Rayner, K. N. (1986). Modeling the diurnal mixed layer. *Limnology and Oceanography, 31*(3), 533-556. https://aslopubs.onlinelibrary.wiley.com/doi/abs/10.4319/lo.1986.31.3.0533
Stainsby, E., Winter, J., Jarjanazi, H., Paterson, A., Evans, D., & Young, J. (2011). Changes in the thermal stability of Lake Simcoe from 1980 to 2008. *Journal of Great Lakes Research, 37*, 55-62.
Stow, C. A., Rowe, M. D., Godwin, C. M., Mason, L. A., Alsip, P. J., Kraus, R. T., et al. (2023). Lake Erie hypoxia spatial and temporal dynamics present challenges for assessing progress toward water quality goals. *Journal of Great Lakes Research, 49*(5), 981-992. https://www.sciencedirect.com/science/article/pii/S038013302300062X
Summers, J. C., Rühland, K. M., Kurek, J., Quinlan, R., Paterson, A. M., & Smol, J. P. (2012). Multiple stressor effects on water quality in Poplar Bay, Lake of the Woods, Canada: a midge-based assessment of hypolimnetic oxygen conditions over the last two centuries. *Journal of Limnology, 71*(1).
Valipour, R., Bouffard, D., & Boegman, L. (2015). Parameterization of bottom mixed layer and logarithmic layer heights in central Lake Erie. *Journal of Great Lakes Research, 41*(3), 707-718.
Verseghy, D. L., & MacKay, M. D. (2017). Offline Implementation and Evaluation of the Canadian Small Lake Model with the Canadian Land Surface Scheme over Western Canada. *Journal of Hydrometeorology, 18*(6), 1563-1582. https://journals.ametsoc.org/view/journals/hydr/18/6/jhm-d-16-0272_1.xml
Walker, R. R., & Snodgrass, W. J. (1986). Model for Sediment Oxygen Demand in Lakes. *Journal of Environmental Engineering, 112*(1), 25-43. https://ascelibrary.org/doi/abs/10.1061/%28ASCE%290733-9372%281986%29112%3A1%2825%29
Wang, X., Huang, G., Lin, Q., & Liu, J. (2014). High-Resolution Probabilistic Projections of Temperature Changes over Ontario, Canada. *Journal of Climate, 27*(14), 5259-5284. https://journals.ametsoc.org/view/journals/clim/27/14/jcli-d-13-00717.1.xml
Wetzel, R. G. (2001). *Limnology: Lake and River Ecosystems*: Academic Press.

Wetzel, R. G. (2023). *Wetzel's Limnology: Lake and river ecosystems* (I. D. Jones & J. P. Smol Eds. 4th ed.): Elsevier.
Woolway, R. I., & Merchant, C. J. (2019). Worldwide alteration of lake mixing regimes in response to climate change. *Nature Geoscience, 12*(4), 271-276. https://doi.org/10.1038/s41561-019-0322-x
Woolway, R. I., Weyhenmeyer, G. A., Schmid, M., Dokulil, M. T., de Eyto, E., Maberly, S. C., et al. (2019). Substantial increase in minimum lake surface temperatures under climate change. *Climatic Change, 155*(1), 81-94. https://doi.org/10.1007/s10584-019-02465-y
Yan, N. D., Paterson, A. M., Somers, K. M., & Scheider, W. A. (2008). An introduction to the Dorset special issue: transforming understanding of factors that regulate aquatic ecosystems on the southern Canadian Shield. *Canadian Journal of Fisheries and Aquatic Sciences, 65*(5), 781-785. https://cdnsciencepub.com/doi/abs/10.1139/f08-077
Yang, B., Young, J., Brown, L., & Wells, M. (2017). High ‐ Frequency Observations of Temperature and Dissolved Oxygen Reveal Under ‐ Ice Convection in a Large Lake. *Geophysical Research Letters, 44*(24).
Yankova, Y., Neuenschwander, S., Köster, O., & Posch, T. (2017). Abrupt stop of deep water turnover with lake warming: Drastic consequences for algal primary producers. *Scientific reports, 7*(1), 13770. https://doi.org/10.1038/s41598-017-13159-9
Yao, Rusak, J. A., Paterson, A. M., Somers, K. M., Mackay, M., Girard, R., et al. (2013). The interplay of local and regional factors in generating temporal changes in the ice phenology of Dickie Lake, south-central Ontario, Canada. *Inland Waters, 3*(1), 1-14. https://www.tandfonline.com/doi/abs/10.5268/IW-3.1.517
Yao, Samal, N. R., Joehnk, K. D., Fang, X., Bruce, L. C., Pierson, D. C., et al. (2014). Comparing ice and temperature simulations by four dynamic lake models in Harp Lake: past performance and future predictions. *Hydrological Processes, 28*(16), 4587-4601. https://onlinelibrary.wiley.com/doi/abs/10.1002/hyp.10180

Supplementary Information

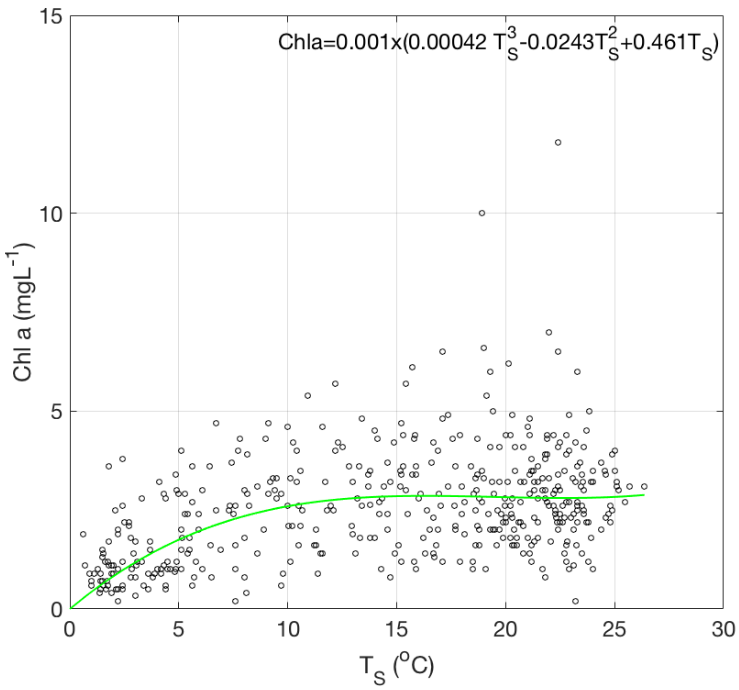

FIG. S1. The relationship between chlorophyll *a* and surface water temperature (solid line) from observations (circles) in Harp Lake.

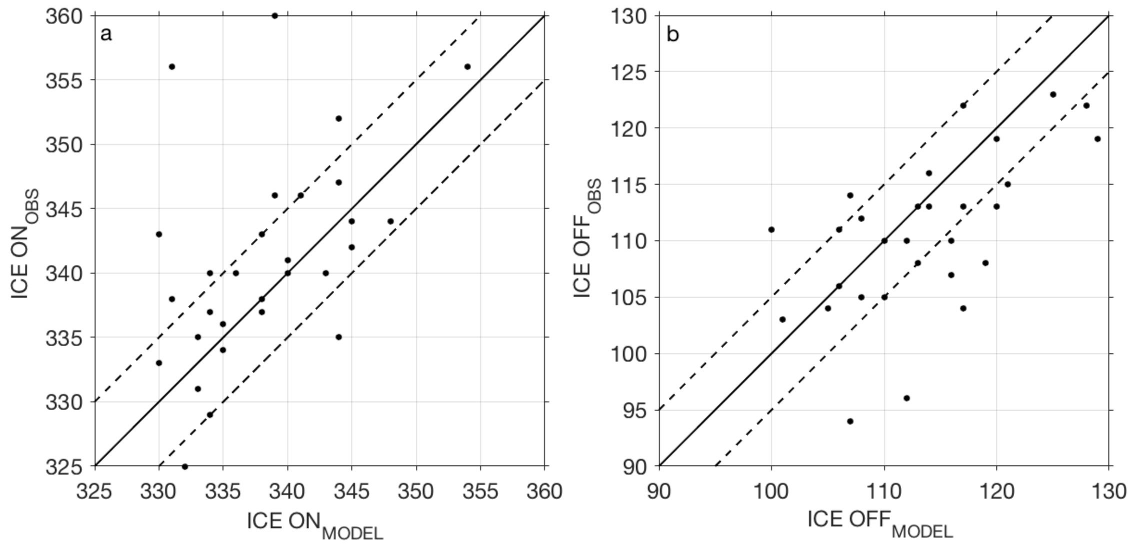

FIG. S2. Comparison of ice on (a; R^2=0.30) and ice off (b; R^2=0.37) between the model and observations in Harp Lake. The dashed lines indicate ±5 days error from model predications equal to observations (the solid line)

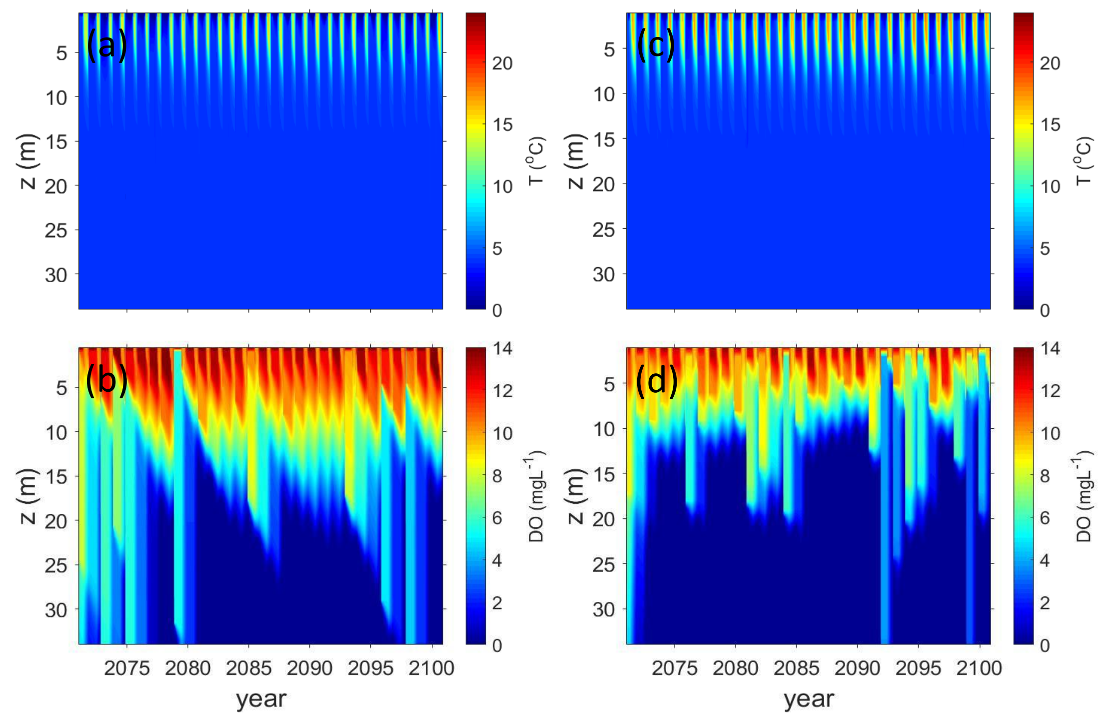

FIG. S3. In Harp Lake, Future prediction time series of water temperature (*T*; a and c) and dissolved oxygen (*DO*; b and d) from global climate model (b and b from RCP 2.6; c and d from RCP 8.5).

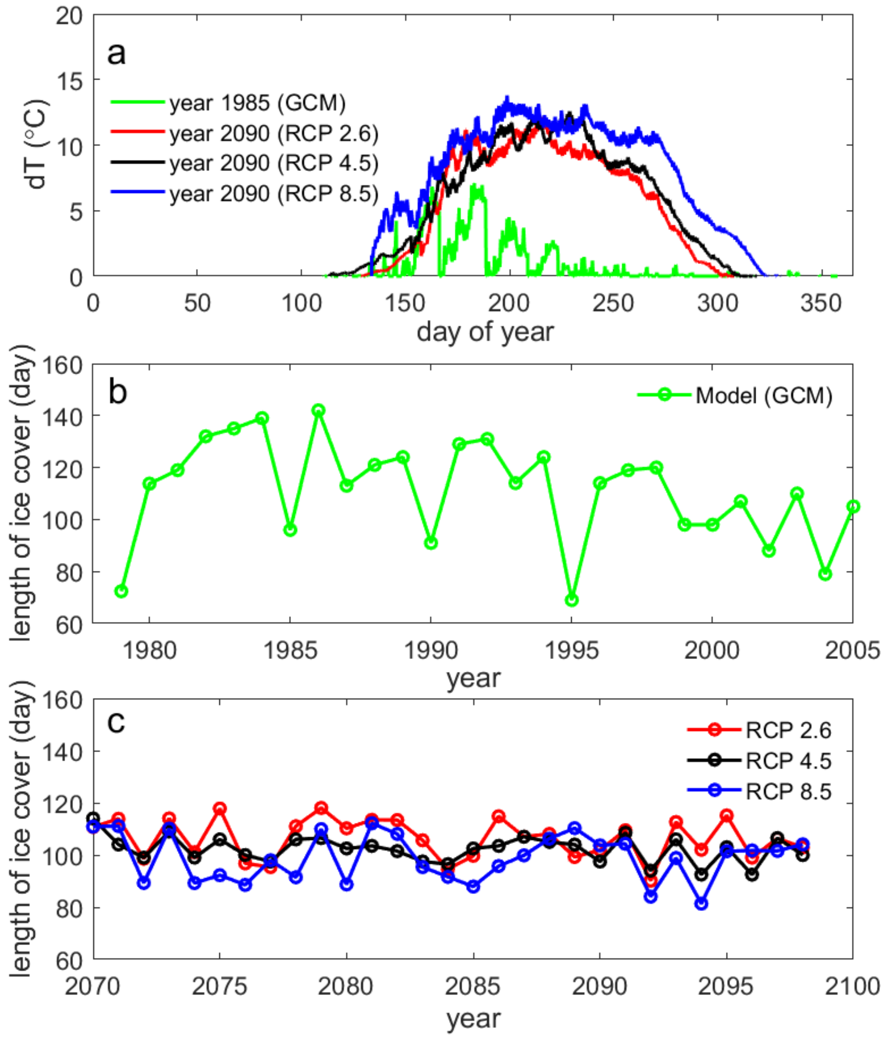

FIG. S4. (a) Simulated temperature difference between the lake surface and the bottom of the metalimnion for a representative future year (2090) and a representative year in the past (1985 in green); GCM simulated historical length of ice cover (b) and future length of simulated ice cover (c).

Table S1: Linear regression results (using fitlm.m in Matlab) for air temperature, VWHO and thermocline depth. Significant trends ($p < 0.05$) are in bold.

Parameter	*p*-value	Slope (parameter y^{-1})	Days Years	Reference
VWHO (mg L^{-1})	**0.0085**	0.034	Sep. 15 1978-2016	Data from Nelligan et al. (2019)
VWHO (mg L^{-1})	0.84	-0.0075	Aug. 15-Sep. 15 1976-1994	Fig. 6c using data from Quinlan et al. (2015)
VWHO (mg L^{-1})	0.34	-0.025	Aug. 15-Sep. 15 1978-2005	Fig. 6c model with GCM forcing
VWHO (mg L^{-1})	0.10	-0.015	Aug. 15-Sep. 15 1978-2005	Fig. 6c model with observed forcing
VWHO (mg L^{-1})	0.30	-0.018	Aug. 15-Sep. 15 1978-2005	Fig. 6c from observation data
Thermocline depth (m)	0.14	-0.011	Sep. 15 1978-2016	Data from Nelligan et al. (2019)
Thermocline depth (m)	0.78	0.0076	Aug. 15-Sep. 15 1979-2005	Fig. 6a model with GCM forcing
Observed air temperature (°C)	**0.0049**	0.10	Aug. 15-Sep. 15 1978-2007	Fig. 4a observed
GCM air temperature (°C)	0.13	0.10	Aug. 15-Sep. 15 1978-2005	Fig. 4a from GCM